

Fractal analysis of the irregular geometry of tensile fracture surface of carbon steels

TAKASHI SAKAI

Department of Mechanical Engineering, Takamatsu National College of Technology, 355 Chokushi, Takamatsu, Kagawa 761-8058 Japan

In this study, tensile tests were carried out on several carbon steels that had been heat-treated using various methods. Their fracture surfaces were observed using scanning laser microscopy. Based on the obtained digital data, an imaginary fracture surface was reconstructed in a three-dimensional (3D) space. Fractal analysis was applied to those 3D surfaces and the Richardson effect was confirmed in the surface irregularity. Finally, it was noted that the geometrical irregularity of the surface is well evaluated by combining the fractal dimension and an additional indices designated as *indices of fracture surface nature*.

(Received February 1, 2007; accepted February 14, 2007)

Keywords: Fractal, Fractal dimension, Richardson effect, Tensile fracture surface, Fractography, Scanning laser microscope, Morphological fracture aspect, Digitized surface, Mechanical property

1. Introduction

To analyze the irregularity of shapes and time-dependent phenomena, many researchers have developed various methods such as Fourier analysis and treatment as stochastic process. The concept of fractals proposed by Mandelbrot [1, 2] is useful to quantify that irregularity. It has therefore been applied successfully in various fields [3–5].

In this study, this fractal concept was applied to evaluate the geometric characteristics of tensile fracture surfaces for pure iron and several carbon steels of S25C, S35C, S45C, and S55C, which had been heat-treated using various methods. The Richardson effect on surface irregularities was confirmed by plotting the $\ln \varepsilon - \ln S$ relationship. In addition, self-similarity was also confirmed within a limited resolution range of the microscopic observation. Based on the current results, the microscopic surface irregularity of the tensile fracture surface was well evaluated by combining the fractal dimension and additional indices: the *indices of fracture surface nature*.

2. Specimens and SLM observation

Materials used in this study were pure iron and carbon steels of S25C, S35C, S45C, and S55C heat-treated variously by annealing, normalizing, quenching, and tempering. Tensile tests were carried out on these specimens, after which the resultant fracture surfaces were observed using scanning laser microscopy (SLM). In contrast to scanning electron microscopy (SEM), SLM can provide three-dimensional (3D) numerical data that are obtained directly in real time: this is a convenience for fractal analysis proposed in this study.

As an example of SLM observation, a micrograph of the tensile fracture surface of normalized S35C steel is shown in Fig. 1 at $500 \times$ magnification. In that micrograph, bright areas indicate a high position on the real surface; dark areas indicate a low position. A square of $948.0 \mu\text{m} \times 948.0 \mu\text{m}$ is defined as a sample space to analyze the fracture surface irregularity. This area is replaced by $200 \text{ dot} \times 200 \text{ dot}$ on a CRT screen. Based on the digital data thus obtained, an imaginary fracture surface was reconstructed in a 3D space. Fig. 1 (b) portrays an example of the resultant imaginary fracture surface. Fractal analysis was performed on the geometrical irregularity of this imaginary fracture surface.

3. Analytical procedure

As reported by one study [4], geometrical irregularity of mechanically finished surfaces was well evaluated using the fractal methods. If a surface has a fractal nature, the following equation between the total area S and measuring unit length ε is applicable:

$$\ln S = \ln F + (2 - D) \ln \varepsilon \quad (1)$$

where D is the fractal dimension calculated from the regression line slope. The value of D is always $D = 2.0$ because the regression line must have a negative slope. The surface area S changes depending on the unit length ε , and the effect of ε on surface area S . This is the so-called *Richardson effect*.

The surface of an irregular body is replaced by a multifaceted surface consisting of numerous triangular facets. Fig. 2 (a) shows that this object corresponds to a plate having an irregular surface if we cut out a certain portion of the body. The irregular surface is replaced here

by a surface derived from 3D numerical data obtained using SLM.

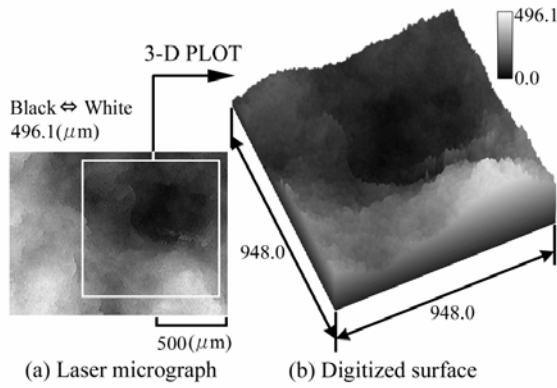


Fig. 1. Laser micrograph and digitized surface of normalized S35C steel.

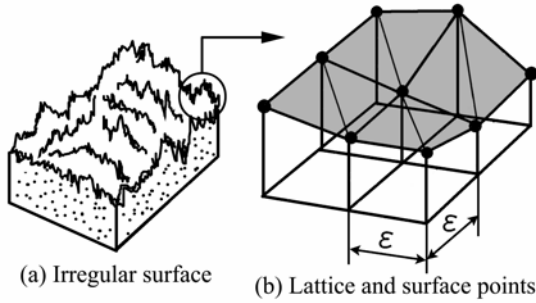


Fig. 2. Replacement of irregular surface by multifacet surface.

Usually, the linear Richardson effect is confirmed within a limited range of ϵ . Therefore, the Richardson effect in the entire region of ϵ should be represented by a different type of expression. The following hyperbola type expression [6] is proposed in this study:

$$(\ln S - E)(\ln S + A \ln \epsilon - B) = C \quad (2)$$

The fractal dimension is calculated from the regression line slope for data points within the linear portion. Meanings of these parameters are indicated schematically in Fig. 3. In this paper, parameters such as B , C and E (except for A) are called *indices of fracture surface nature* because these parameters well reflect the geometric characteristics of the fracture surface. The index of a fracture surface nature E provides the area of a perfect surface. If the fracture surface is perfectly flat, then $D=2.0$. The decrease of the another index, C , corresponds to the expansion of the region in which the linear Richardson effect is observed. The index of $(B-E)/A$ provides the value of $\ln \epsilon$ at the intersection of two dashed lines. Here, C is standardized as

$$C^* = y_c / E \quad (3)$$

where y_c is the value on the regression line at $\ln \epsilon = (B-E)/A$.

4. Analytical results and discussion

4.1 Effect of SLM magnification

The relationships between $\ln \epsilon$ and $\ln S$ obtained for the fracture surfaces of normalized S35C steel are shown in Fig. 4. Fractal dimensions and each index of the fracture surface nature obtained from SLM micrographs are listed in Table 1. In Fig. 4, each solid line is determined to provide the least-squares values for data points along the sloped portion. Fractal dimensions for respective magnifications are calculated from each regression line's slope. Each dashed line indicates the level of a perfect flat surface for the corresponding magnification.

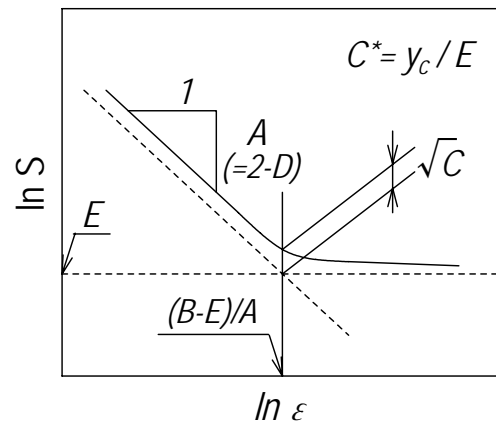


Fig. 3. Schematics of $\ln \epsilon$ - $\ln S$ relationship.

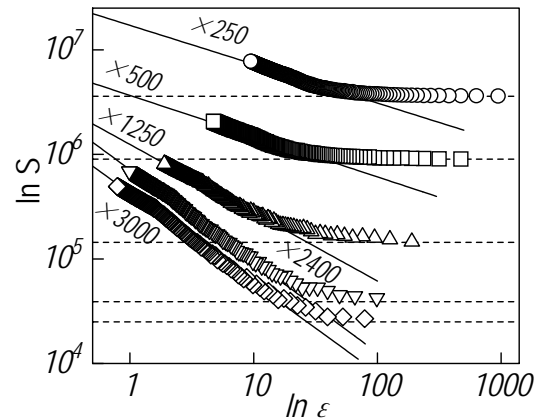


Fig. 4. $\ln \epsilon$ - $\ln S$ relationships for normalized S35C carbon steels.

If the analytical object has a fractal nature, then the irregularity is well evaluated using the fractal dimension. However, that value depends on the magnification, as depicted in Fig. 5, where dimension D remains constant in Region I. Consequently, self-similarity is confirmed on the fracture surface observed at magnification higher than $2000\times$. A similar trend was apparent for fracture surfaces of other types of steels examined in this study.

Table 1. Numerical list of analytical results.

Material	Mag.	Mark	D	$B-E/A$	C^*
	250	○	2.372	67.15	1.076
	500	□	2.389	36.68	1.109
S35C	1250	△	2.653	27.07	1.336
	2400	▽	2.875	27.77	1.369
	3000	◇	2.860	27.01	1.378

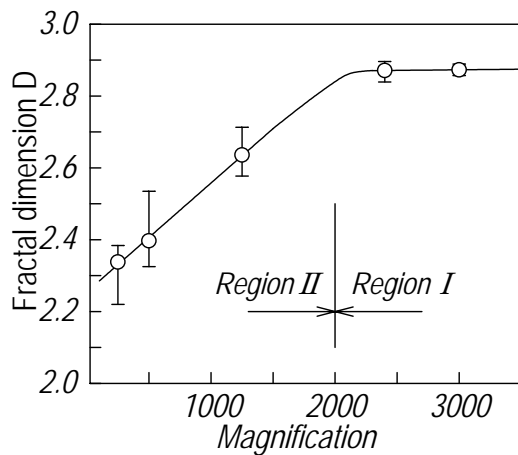


Fig. 5. Magnification vs. fractal dimension for normalized S35C steels.

4.2 Effects of carbon content

The effect of carbon contents in the steels on the fracture surface irregularity was examined: those analytical results are shown in Fig. 6. The fractal dimension is presumed to be constant for every kind of steel because the regression line slope is the same. This fact indicates that the carbon content has no effect on the fractal dimension. In this figure, the respective results appear as $S55C < S45C < S25C < PI$ (pure iron). Therefore, the intersection of the regression line is inversely proportional to the carbon content. Similarly, the value of $(B-E)/A$ tends to decrease with increased carbon content.

4.3 Effect of mechanical properties

As shown in Fig. 6, the value of $(B-E)/A$ tends to decrease with increased strength. This aspect is indicated

schematically in Fig. 7. Results for high-strength steel are plotted as ●; the results for low-strength steel (or pure iron) are shown as ○. The regression line for the sloped portion in the former case appears on the left-hand side compared with the result for the latter case. This fact indicates that the fractal nature of the fracture surface for the high-strength steel is realized in the low level of ϵ . In other words, the value of $(B-E)/A$ tends to decrease as the strength level is increased. Morphological interpretation for the fracture surface is also attached to Fig. 7. The result for high-strength steel (a) gives the low value of $(B-E)/A$ and the microscopic irregularity of the fracture surface, whereas the result for low-strength steel (b) provides a high value of $(B-E)/A$ and macroscopic irregularity.

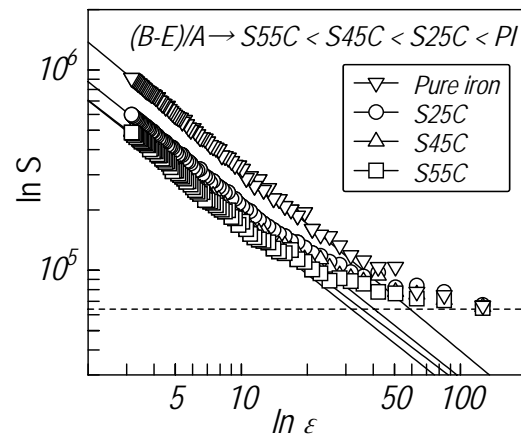


Fig. 6. $\ln \epsilon - \ln S$ relationships for several carbon steels.

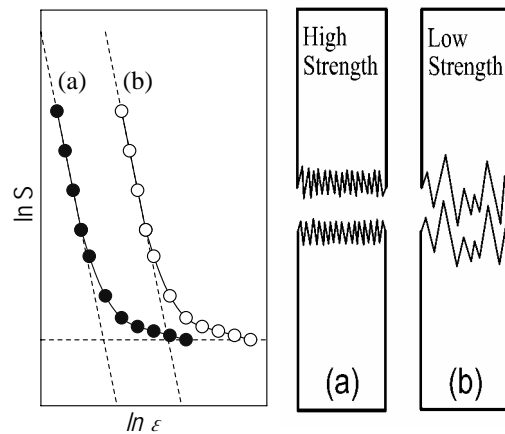


Fig. 7. Correspondence of $(B-E)/A$ to morphological fracture aspect.

4. Conclusions

Analytical procedures to evaluate the surface irregularity of the tensile fracture surfaces for several

carbon steels were developed by applying the fractal concept and a curve-fitting technique. The main conclusions obtained through this study are summarized as follows.

- (1) The tensile fracture surfaces for pure iron and carbon steels of S25C, S35C, S45C, and S55C that have been heat-treated with various methods have a fractal nature.
- (2) The results show that the geometrical irregularities of the fracture surface can be well evaluated by combining the fractal dimension and additional indices governed by carbon content and mechanical properties.
- (3) The index of $(B-E)/A$ is closely related to fracture mechanisms and the strength level of a material.

References

- [1] B. B. Mandelbrot, *The Fractal Geometry of Nature*, W. H. Freeman and Company, (1983).
- [2] B. B. Mandelbrot, *Fractals: Form, Chance and Dimension*, W. + H. Freeman and Company, (1977).
- [3] M. Tanaka, *Journal of Materials Science Research International, Japan*, **47**, 169 (1998).
- [4] T. Sakai, T. Sakai, A. Ueno, *Transaction of Japan Society of Mechanical Engineering, A-64*, 620 (1998).
- [5] T. Sakai, M. Fujikawa, S. L. McIntyre, R. C. Bradt, *Journal of Materials Science Research International*, **41**, 470 (1992).
- [6] S. Nishijima, *Transaction of Japan Society of Mechanical Engineering, A-46*, 412 (1990).

*Corresponding author: sakai@takamatsu-nct.ac.jp